Emergence of exotic electronic and magnetic phases under electron filling in Na_2BO_3 (B=Ta,Ir,Pt,Tl): A first-principles study†

Priyanka Yadav[a], Sumit Sarkar[a], Deodatta Moreshwar Phase[a] and Rajamani Raghunathan[a,*]

Supporting Information

1 Methods

All the calculations have been performed within the DFT framework as implemented in the Vienna Ab initio Simulation Package using PAW pseudopotentials[1–4]. Electron configurations of $5p^6 5d^4 6s^1$ for Ta, $5d^8 6s^1$ for Ir, $5d^9 6s^1$ for Pt, $5d^{10} 6s^2 6p^1$ for Tl; $2p^6 3s^1$ for sodium; and $2s^2 2p^4$ for oxygen were treated as valence electrons. The starting structures for the calculations have been obtained from the previously reported crystal structures of Na_2IrO_3 with $C2/m$ and $C2/c$ space groups[5,6]. These structures have relaxed both in terms of volume and ion positions to determine the ground state structure. The wave function for the valence electrons has been expanded using plane waves with an energy cutoff of 600 eV. To account for the strong correlations of the 5*d* electrons, the GGA+U formalism has been employed, using the simplified rotationally invariant approach introduced by Dudarev and coworkers[7] by setting U values, namely 1.2, 1.7, and 2.4 eV with $J = 0.6$ eV. In all the calculations SOI has been included. During structural relaxation, a force tolerance of 5 meV/Å and an energy tolerance of 10^{-8} eV have been enforced. In case of phonon calculations, a more stringent force tolerance of 5 x 10^{-3} meV/Å was used. The Brillouin zone integration has been performed using a k-point grid of 6x4x6 for the $C2/m$ and 6x4x4 for the $C2/c$ space groups. Bader charges have been calculated using the Henkelman's code[8–11]. The charge densities were visualized using the VESTA software. Maximally localized Wannier functions (MLWFs) have been calculated by using the Wannier 90 code[12,13].

Electron localisation function (ELF) is estimated from the excess kinetic energy in the fermionic limit (D_f) as compared to the bosonic or non-interacting picture (D_b)[14]. ELF is given by,

$$\begin{aligned} ELF &= \frac{1}{1+\left(\frac{D_f}{D_b}\right)^2} \\ D_f &= \frac{1}{2}\sum_i |\nabla\phi_i|^2 - \frac{1}{8}\frac{|\nabla\rho|^2}{\rho} \\ D_b &= \frac{3}{10}(3\pi^2)^{5/3}\rho^{5/3} \end{aligned} \quad (1)$$

where, ρ is the electron or charge density and ϕ_i's are the Kohn-Sham orbitals. ELF represents the probability of finding an electron in the vicinity of another electron with the same spin and can take values between 0 and 1.

2 Supporting tables:

[a] UGC-DAE Consortium for Scientific Research, D.A.V.V. campus, Khandwa Road, Indore 452001, Madhya Pradesh, India. E-mail: rajamani@csr.res.in

Table S1 Energies (ΔE) of NBO for respective space groups with their structural, electronic and magnetic parameters within the GGA+SO+U formalism for U=0.0 eV.

System	Space group	Energy (meV/f.u.)	Magnetic ground state	Relaxed cell parameters (a, b, c, β)	Angular momentum (s_x, s_y, s_z) $\vert\vec{s}\vert$; (l_x, l_y, l_z) $\vert\vec{l}\vert$	Band gap (eV)
Na_2TaO_3	$C2/c$	0.0	NM	5.39, 9.52, 11.32 and 98.11°	NM	0.79
	$C2/m$	366.0	FM	5.44, 9.39, 5.85 and 108.21°	Ta:(0.17,0.01,0.08) 0.19; (0.10,0.01,0.08) 0.13	metal
Na_2IrO_3	$C2/c$	7.0	ZZ	5.56, 9.59, 10.75 and 99.54°	Ir:(0.04,0.00,0.16)0.18; (0.12,0.00,0.21) 0.24	0.096
	$C2/m$	0.0	ZZ	5.54, 9.59, 5.65 and 109.03°	Ir:(0.09,0.0,0.14) 0.17; (0.19,0.0,0.17) 0.24	0.11
Na_2PtO_3	$C2/c$	0.0	NM	5.51, 9.55, 10.81 and 99.50°	NM	1.32
	$C2/m$	1.0	NM	5.51, 9.54, 5.65 and 109.29°	NM	1.30
Na_2TlO_3	$C2/c$	0.0	FM	5.83, 10.10, 11.41 and 99.82°	O:(0.00,0.00,0.14) 0.14; (0.00,0.00,0.00) 0.00	metal
	$C2/m$	1.0	FM	5.84, 10.10, 5.95 and 109.23°	O:(0.00,0.00,0.14) 0.14; (0.00,0.00,0.00) 0.00	metal

Table S2 Energies (ΔE) of NBO for respective space groups with their structural, electronic and magnetic parameters within the GGA+SO+U formalism for U=1.2 eV.

System	Space group	Energy (meV/f.u.)	Magnetic ground state	Relaxed cell parameters (a, b, c, β)	Angular momentum (s_x, s_y, s_z) $\vert\vec{s}\vert$; (l_x, l_y, l_z) $\vert\vec{l}\vert$	Band gap (eV)
Na_2TaO_3	$C2/c$	0.0	NM	5.39, 9.52, 11.32 and 98.11°	NM	0.71
	$C2/m$	360.0	FM	5.44, 9.39, 5.85 and 108.21°	Ta:(0.09, 0.00, 0.31) 0.32; (0.02, 0.00, 0.07) 0.07	metal
Na_2IrO_3	$C2/c$	1.0	ZZ	5.56, 9.59, 10.75 and 99.54°	Ir:(0.05, 0.00, 0.16) 0.17; (0.15, 0.00, 0.25) 0.29	0.26
	$C2/m$	0.0	ZZ	5.52, 9.58, 5.63 and 109.03°	Ir:(0.10, 0.0, 0.14) 0.17; (0.23, 0.00, 0.19) 0.3	0.25
Na_2PtO_3	$C2/c$	0.0	NM	5.51, 9.54, 10.80 and 99.50°	NM	1.41
	$C2/m$	0.0	NM	5.51, 9.54, 5.65 and 109.29°	NM	1.40
Na_2TlO_3	$C2/c$	0.0	FM	5.84, 10.10, 11.41 and 99.82°	O:(0.00,0.00,0.15) 0.15; (0.00,0.00,0.00) 0.00	metal
	$C2/m$	0.0	FM	5.84, 10.10, 5.95 and 109.23°	O:(0.00,0.00,0.14) 0.14; (0.00,0.00,0.00) 0.00	metal

Table S3 Energies (ΔE) of NBO for respective space groups with their structural, electronic and magnetic parameters within the GGA+SO+U formalism for U=2.4 eV.

System	Space group	Energy (meV/f.u.)	Magnetic ground state	Relaxed cell parameters (a, b, c, β)	Angular momentum (s_x, s_y, s_z) $\vert\vec{s}\vert$; (l_x, l_y, l_z) $\vert\vec{l}\vert$	Band gap (eV)
Na_2TaO_3	$C2/c$	0.0	NM	5.40, 9.52, 11.32 and 98.11°	NM	0.83
	$C2/m$	320.0	FM	5.44, 9.40, 5.86 and 108.21°	Ta:(0.11, 0.00, 0.31) 0.33; (0.01, 0.00, 0.04) 0.04	0.11
Na_2IrO_3	$C2/c$	4.0	ZZ	5.56, 9.60, 10.75 and 99.54°	Ir:(0.05, 0.00, 0.17) 0.18; (0.20, 0.00, 0.30) 0.36	0.67
	$C2/m$	0.0	ZZ	5.56, 9.59, 5.62 and 109.64°	Ir:(0.11,0.00,0.14) 0.17; (0.30, 0.0, 0.22) 0.37	0.66
Na_2PtO_3	$C2/c$	0.0	NM	5.51, 9.55, 10.81 and 99.50°	NM	1.57
	$C2/m$	0.0	NM	5.51, 9.54, 5.65 and 109.29°	NM	1.57
Na_2TlO_3	$C2/c$	0.0	FM	5.84, 10.10, 11.41 and 99.82°	O:(0.00,0.00,0.14) 0.14; (0.00,0.00,0.00) 0.00	metal
	$C2/m$	0.0	FM	5.84, 10.10, 5.95 and 109.23°	O:(0.00,0.00,0.14) 0.14; (0.00,0.00,0.00) 0.00	metal

Table S4 Energies (ΔE) of NBO under four possible magnetic configurations calculated using GGA+SO+U method with U=1.7 eV for $C2/m$ structure.

Na_2BO_3	FM (meV/f.u.)	Zigzag (meV/f.u.)	Néel (meV/f.u.)	Stripy (meV/f.u.)
Na_2TaO_3	0.0	2.5	20.7	4.8
Na_2IrO_3	3.0	0.0	6.9	6.2
Na_2TlO_3	0.0	22.5	54.0	70.0

Table S5 Energies (ΔE) of NBO under four possible magnetic configurations calculated using GGA+SO+U method with U=1.7 eV for $C2/c$ structure.

Na_2BO_3	FM (meV/f.u.)	Zigzag (meV/f.u.)	Néel (meV/f.u.)	Stripy (meV/f.u.)
Na_2IrO_3	4.0	0.0	1.8	7.1
Na_2TlO_3	0.0	24.0	55.0	71.0

3 Supporting Figures

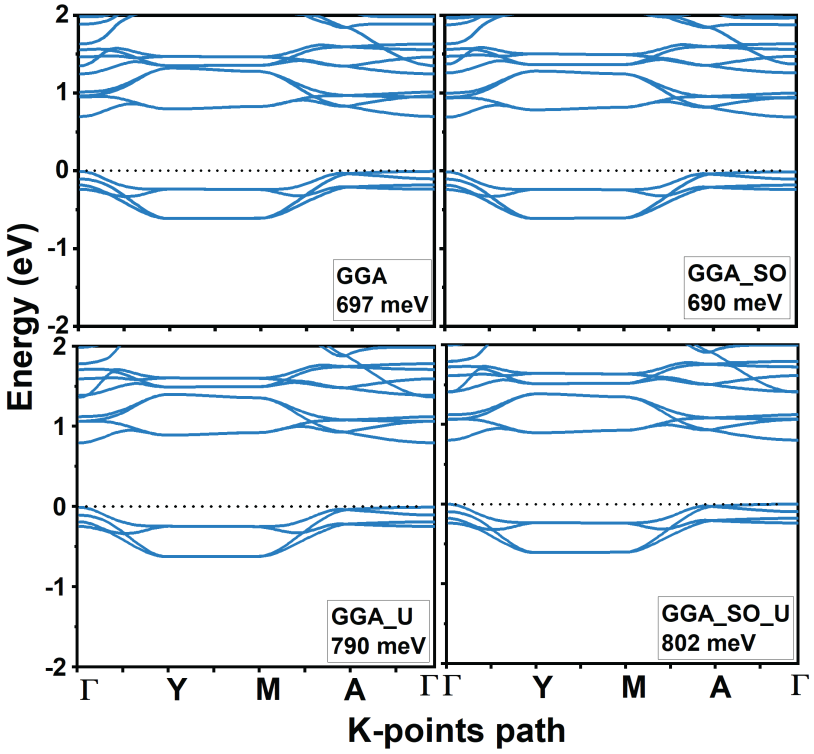

Fig. S1 Band dispersion plot using GGA, GGA+SO, GGA+U, and GGA+SO+U methodology representing the minor role of SOI on the electronic structure in NTO.

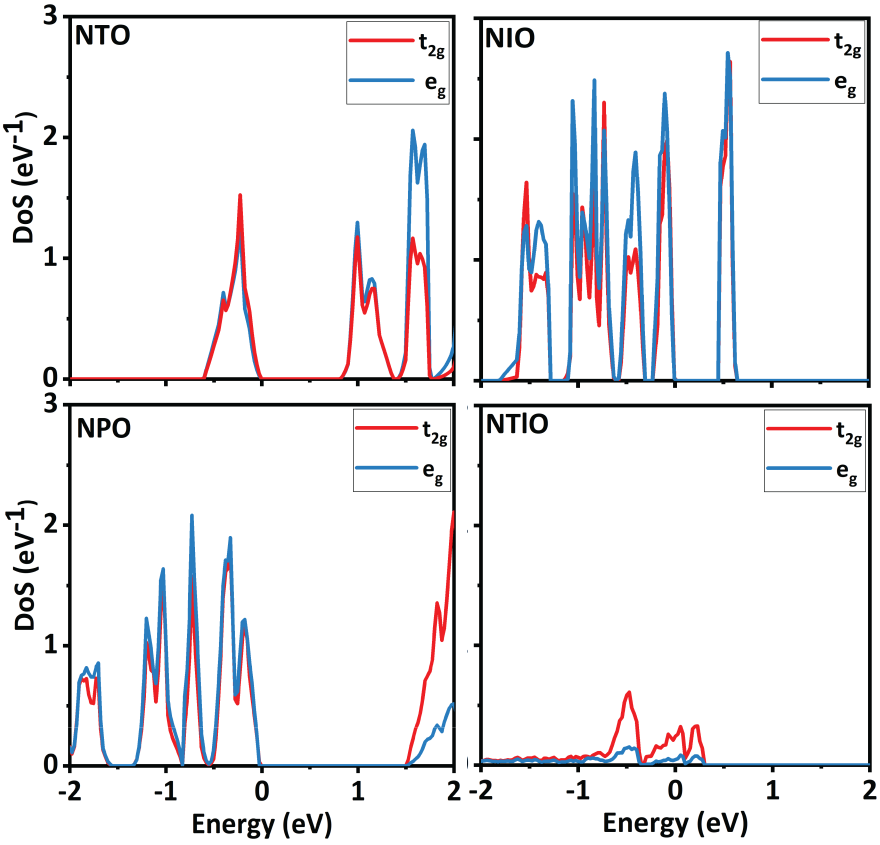

Fig. S2 Projected DoS plots for all the NBO compounds for their respective ground states under GGA+SO+U formalism with U=1.7 eV.

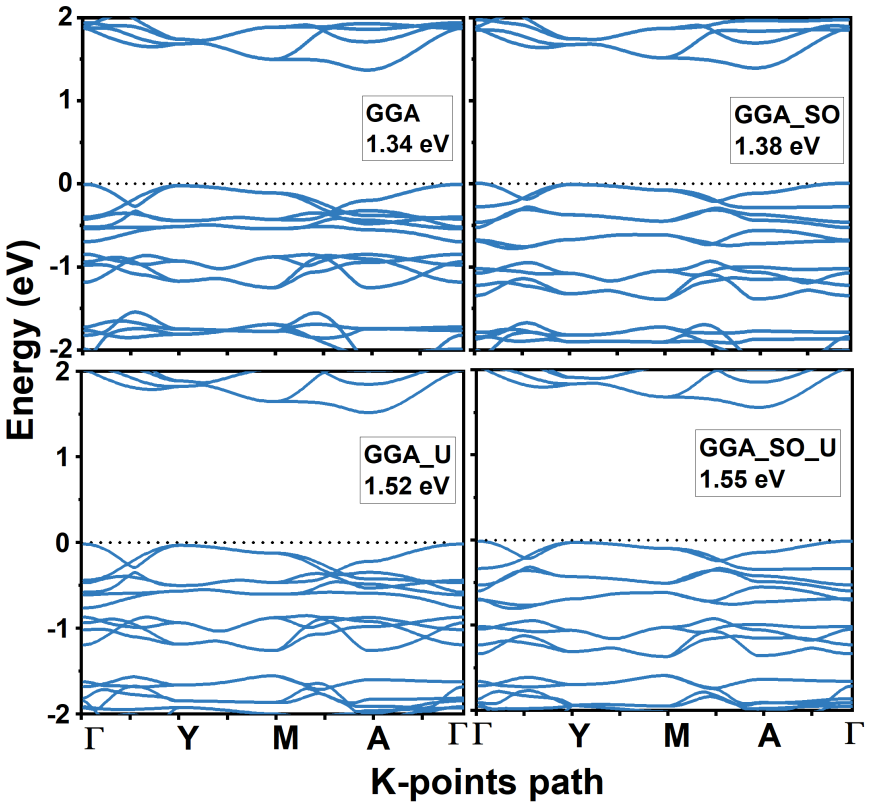

Fig. S3 Band dispersion plot using GGA, GGA+SO, GGA+U, and GGA+SO+U methodology representing the insignificant role of U and SOI in the description of the electronic ground state of NPO.

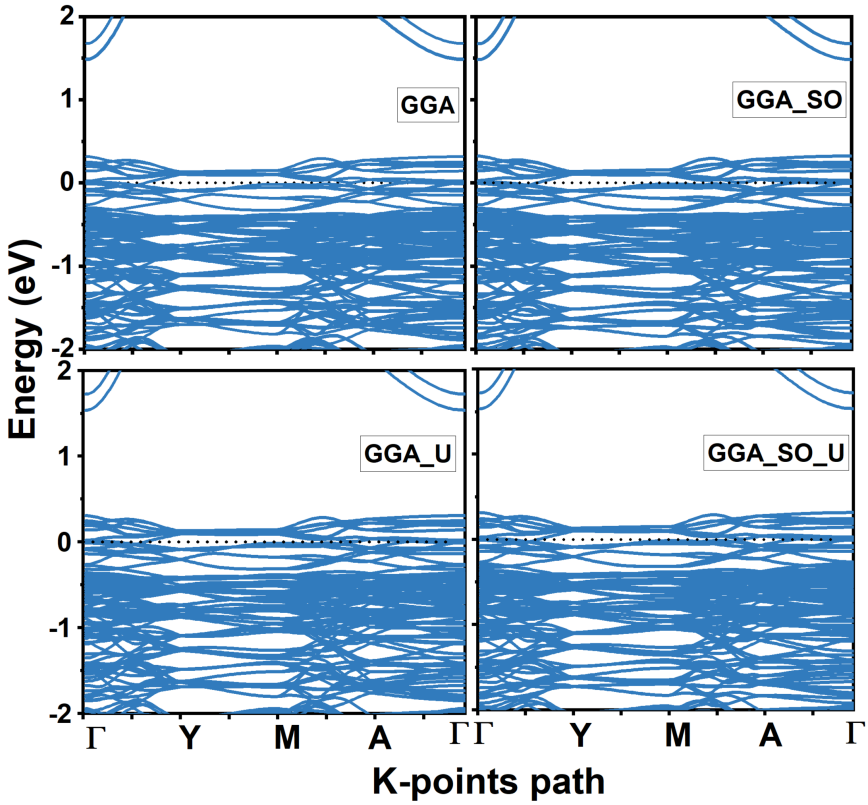

Fig. S4 Band dispersion plot for NTIO using GGA, GGA+SO, GGA+U, and GGA+SO+U methodology representing almost identical electronic structure is obtained across all the four formalisms.

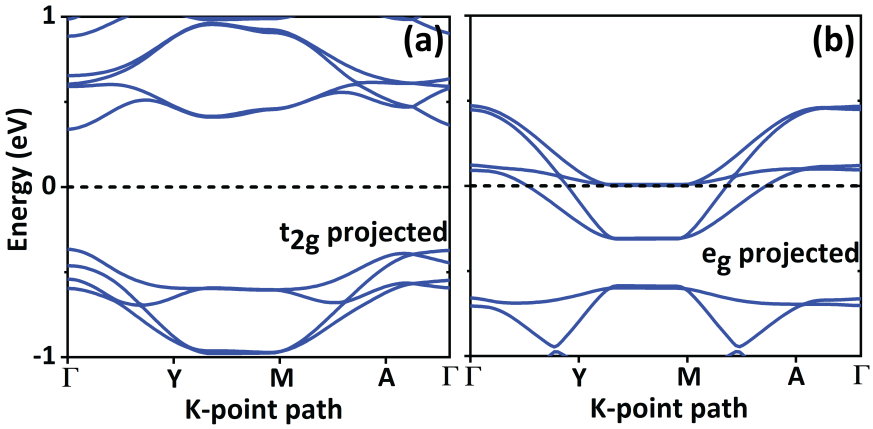

Fig. S5 Wannier projected band on t_{2g} and e_g orbitals showing (a) t_{2g} orbitals show band dispersion similar with DFT calculated band and shows insulating gap due to σ bonding (b) metallic band in e_g due to π bonding.

4 Dynamical stability

In order to investigate the dynamical stability, we have performed phonon dispersion calculations for the respective ground state structures. These calculations allow us to analyze the behavior of the crystal lattice in terms of its vibrational modes. The resulting dispersion curves, obtained along different high symmetry **q**-paths, are presented in figure S6. Generally, the presence of negative phonon frequency in the dispersion curve indicates a structural instability or lattice distortion. Our calculated dispersion curves for all the four compounds do not exhibit any significant negative phonon frequency. The small negative frequency observed in Na_2TlO_3 at the Γ point could be attributed to numerical inaccuracy[15]. These observations suggest that the NBO compounds are structurally stable. We observe a triply degenerate phonon mode of zero frequency at the Γ point which disperse linearly with **q**. These modes correspond to the displacement of the unit cell along the three crystallographic axes, known as the accoustic modes. No gap is observed between the accoustic and optical phonon modes for all the four compounds. However, the longitudinal (LO) and transverse optical (TO) phonon modes are separated by a finite gap in the semiconducting compounds viz., NTO, NIO and NPO and no LO-TO splitting is seen in NTlO.

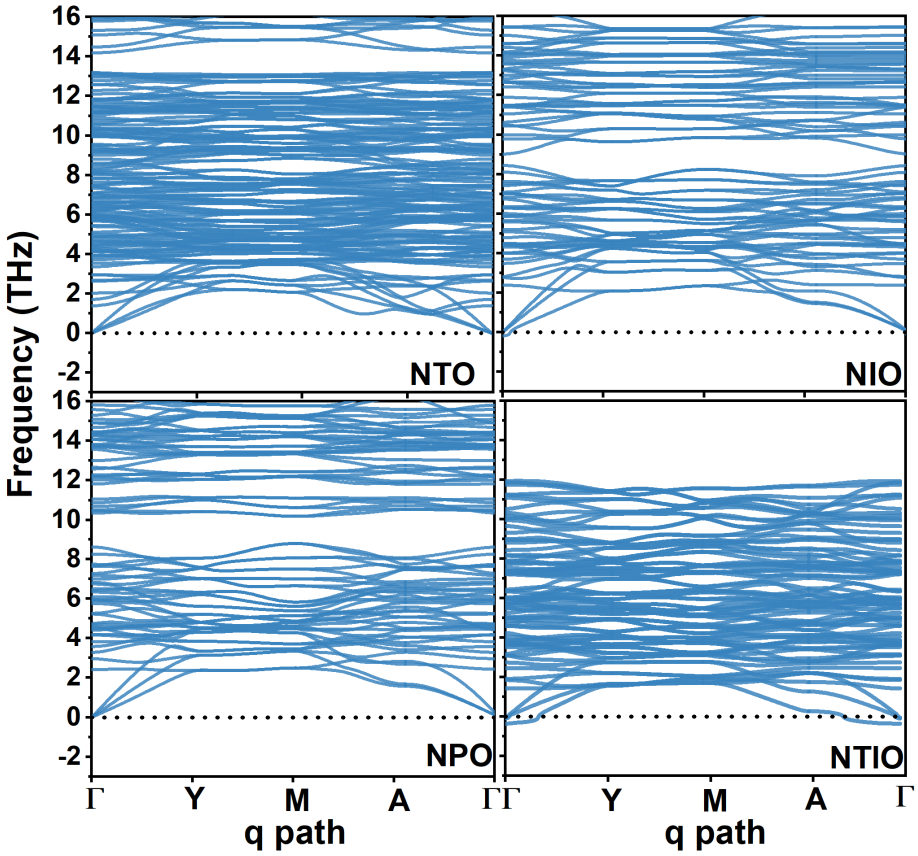

Fig. S6 Dynamical stability of NBO compositions for respective ground states demonstration all the structures are dynamically stable with positive vibrational frequencies.

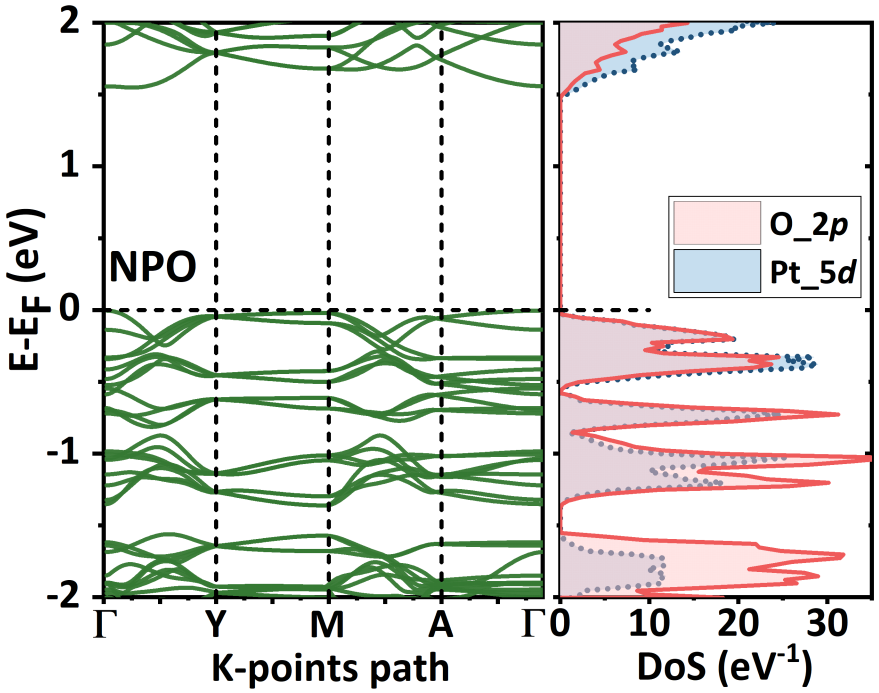

Fig. S7 Band structure of NPO with $C2/c$ symmetry.

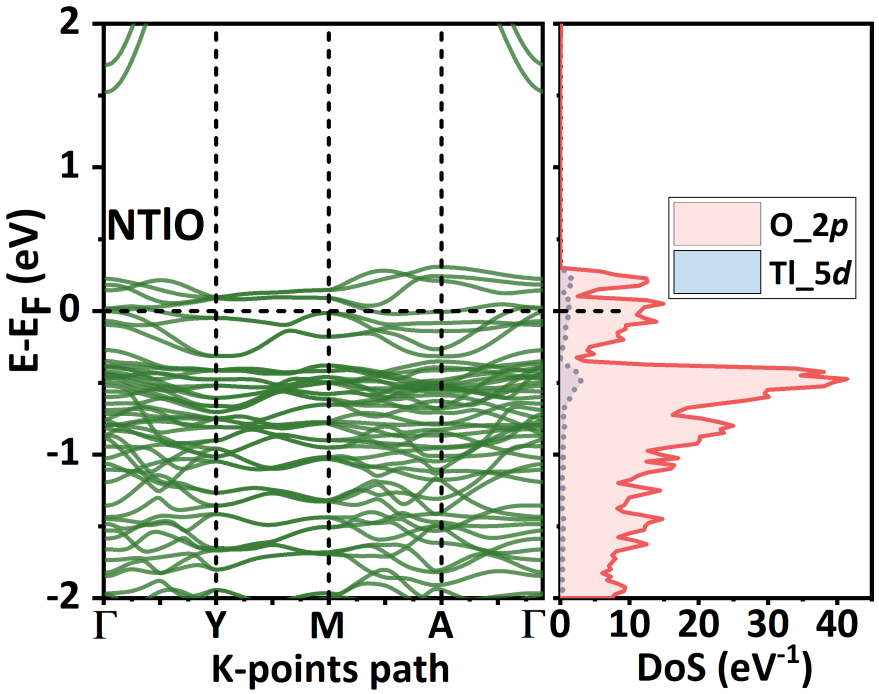

Fig. S8 Band structure of NTlO with $C2/m$ symmetry.

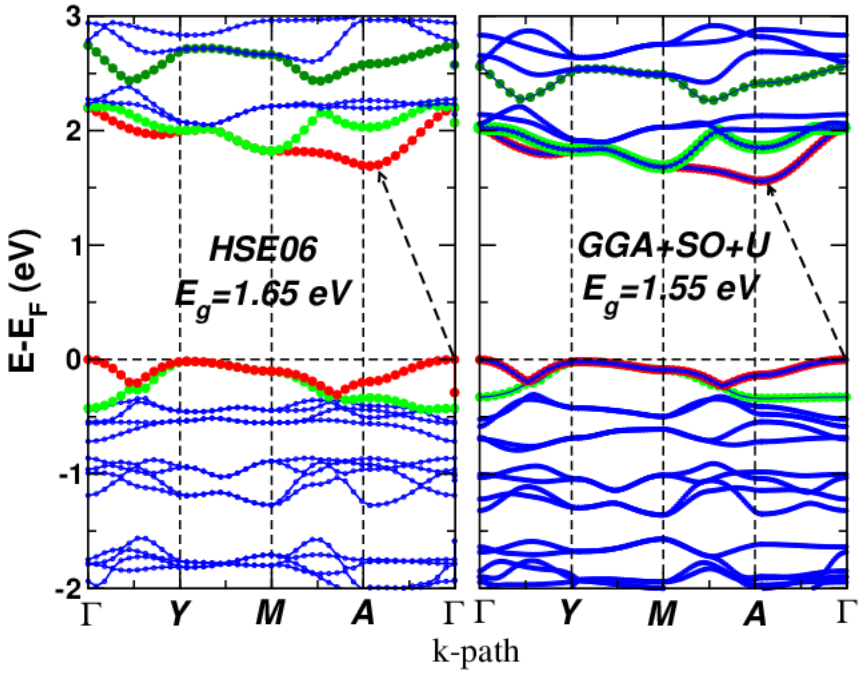

Fig. S9 Comparison of band structures of NPO calculated using HSE06 and GGA+SO+U methods.

Notes and references

1 G. Kresse and J. Hafner, *Phys. Rev. B*, 1993, **48**, 13115–13118.
2 G. Kresse and J. Hafner, *Phys. Rev. B*, 1994, **49**, 14251–14269.
3 G. Kresse and J. Furthmüller, *Phys. Rev. B*, 1996, **54**, 11169–11186.
4 P. E. Blöchl, *Phys. Rev. B*, 1994, **50**, 17953–17979.
5 Y. Singh and P. Gegenwart, *Phys. Rev. B*, 2010, **82**, 064412.
6 S. K. Choi, R. Coldea, A. N. Kolmogorov, T. Lancaster, I. I. Mazin, S. J. Blundell, P. G. Radaelli, Y. Singh, P. Gegenwart, K. R. Choi, S.-W. Cheong, P. J. Baker, C. Stock and J. Taylor, *Phys. Rev. Lett.*, 2012, **108**, 127204.
7 S. L. Dudarev, G. A. Botton, S. Y. Savrasov, C. J. Humphreys and A. P. Sutton, *Phys. Rev. B*, 1998, **57**, 1505–1509.
8 E. Sanville, S. Kenny and R. Smith, *Journal of computational chemistry*, 2007, **28**, 899–908.
9 E. Sanville, S. D. Kenny, R. Smith and G. Henkelman, *Journal of Computational Chemistry*, 2007, **28**, 899–908.
10 W. Tang, E. Sanville and G. Henkelman, *Journal of Physics: Condensed Matter*, 2009, **21**, 084204.
11 G. Henkelman, A. Arnaldsson and H. JÃşnsson, *Computational Materials Science*, 2006, **36**, 354–360.
12 A. A. Mostofi, J. R. Yates, Y.-S. Lee, I. Souza, D. Vanderbilt and N. Marzari, *Computer Physics Communications*, 2008, **178**, 685–699.
13 N. Marzari, A. A. Mostofi, J. R. Yates, I. Souza and D. Vanderbilt, *Rev. Mod. Phys.*, 2012, **84**, 1419–1475.
14 B. Silvi and A. Savin, *Nature*, 1994, **371**, 683–686.
15 I. Pallikara, P. Kayastha, J. M. Skelton and L. D. Whalley, *Electronic Structure*, 2022, **4**, 033002.